Prevention of Apoptosis by a Baculovirus Gene During Infection of Insect Cells

ROLLIE J. CLEM, MARCUS FECHHEIMER, LOIS K. MILLER*

Programmed cell death is an active process of self destruction that is important in both the development and maintenance of multicellular animals. The molecular mechanisms controlling activation or suppression of programmed cell death are largely unknown. Apoptosis, a morphologically and biochemically defined type of programmed cell death commonly seen in vertebrates, was found to be initiated during baculovirus replication in insect cells. A specific viral gene product, p35, was identified as being responsible for blocking the apoptotic response. Identification of the function of this gene will allow further definition of the molecular pathways involved in the regulation of programmed cell death and may identify the role of apoptosis in invertebrate viral defense systems.

APOPTOSIS IS A MAJOR MECHANISM of physiologically relevant cell death in vertebrates. Cells undergoing apoptosis generate membrane-bound subcellular apoptotic bodies and activate an endogenous nuclease that cleaves the cellular chromatin DNA into discrete fragments. Apoptosis is ascribed roles in processes as diverse as embryogenesis, tumor regression, and cytolytic T cell–directed killing of virally infected cells (*1–5*). Programmed cell death also participates in insect development and tissue homeostasis (*6–9*), although chromatin digestion, the biochemical hallmark of apoptosis, has not been documented in invertebrate programmed cell death.

Our observation of apoptosis in baculovirus-infected insect cells arose during the characterization of a mutant of the baculovirus *Autographa californica* multiply-embedded nuclear polyhedrosis virus (AcMNPV). AcMNPV possesses a 128-kb circular DNA genome that replicates in the nucleus of its insect host cell (*10*). The infection is lytic; cell lysis normally occurs 72 or more hours after infection, after the virus particles are embedded in proteinaceous polyhedral occlusion bodies. During routine expression vector screening, the viral mutant, named the annihilator (vAcAnh), was isolated as a small plaque lacking occlusion bodies. In initial studies, vAcAnh was used to infect cell lines derived from three different species of lepidopteran insects. The mutant caused premature death of *Spodoptera frugiperda* (SF-21) (*11*) and *Bombyx mori* (BmN-4) (*12*) cells but not *Trichoplusia ni* (TN-368) (*13*) cells. We therefore propagated and titered vAcAnh using the TN-368 cell line.

The vAcAnh mutation was mapped by marker rescue to the AcMNPV Eco RI-S fragment (Fig. 1A), which contains the entire *p35* gene and a portion of the *p94* gene (*14*). The Eco RI-S fragment of vAcAnh was cloned and partially sequenced. A 754–base pair deletion was found that would result in the truncation of p35 by the removal of 132 amino acids from the carboxyl terminus and the addition of ten amino acids acquired by fusion into the adjacent hr5 region (Fig. 1, B and C).

To confirm that the deletion of vAcAnh in *p35* was responsible for the annihilator phenotype, we inactivated *p35* of wild-type AcMNPV by inserting the *Escherichia coli lacZ* gene (Fig. 1B), resulting in the recombinant virus vP35Z. The phenotype of vP35Z is identical to that of vAcAnh (below), a result that indicates the presence of the intact *p35* gene is required to prevent premature death of AcMNPV-infected SF-21 cells.

SF-21 cells infected with wild-type AcMNPV and vAcAnh were examined by microscopy (Fig. 2). During a wild-type AcMNPV infection, small protrusions transiently appeared on the surface of the infected cells approximately 12 hours after infection (Fig. 2B). These protrusions normally disappeared, and by 24 hours occlusion bodies were visible in the nuclei. Cells infected with wild-type virus remained intact for 72 hours or more. This transient blebbing at 12 hours did not occur in TN-368 cells infected with either wild-type or vAcAnh (*15*). In vAcAnh-infected SF-21 cells, protrusions appeared on the surface of the cells (Fig. 2C) that were similar to protrusions observed in a wild-type infection. However, instead of disappearing with time, the blebbing process intensified and large, membrane-bound bodies arose and separated from the cells (Fig. 2D). The nucleus and cytoplasm of an affected cell were sectioned into these bodies until only a cluster of bodies remained. For an individual cell, the entire process of disintegration required approximately 1 to 2 hours. The subcellular bodies, which are morphologically similar to apoptotic bodies, remained over the next few days.

The mitochondria of blebbing cells remained functionally intact during the blebbing process. Staining with rhodamine 123, which accumulates in mitochondria with an active membrane potential (*16*), revealed energized mitochondria in the blebbing cells and in some of the bodies themselves (Fig. 2, E and F). Our results are similar to those of previous studies, which showed morphologically intact mitochondria in apoptotic cells and apoptotic bodies (*2–4*). These results suggest that the cells are undergoing an active process of cell death.

The nuclei of vAcAnh-infected SF-21 cells broke up into small fragments during the blebbing process (Fig. 2, G and H), and nuclear fragments were present in some of the bodies released by the dying cell. This type of nuclear disintegration is also observed in the process of apoptosis (*2–4*).

Because the morphological evidence (Fig. 2) indicated that vAcAnh-infected SF-21

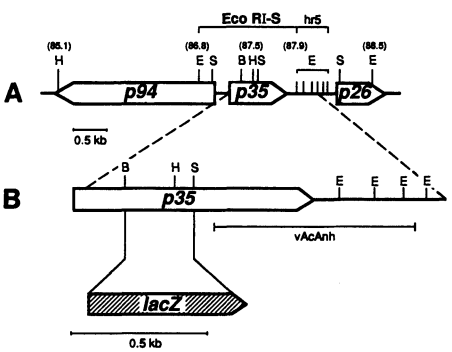

Fig. 1. Mapping and sequencing of the vAcAnh mutation and construction of vP35Z, the *p35-lacZ* insertion mutant (*24*). (**A**) Partial genome map of AcMNPV. The three major open reading frames in the region, which encode p94, p35, and p26 are indicated by arrows. Numbers in parentheses represent map units on the AcMNPV genome. The hr5 region is one of six homologous regions in the AcMNPV genome that are highly repetitive and contain multiple Eco RI sites (*25*). The restriction sites are as follows: B, Bcl I; E, Eco RI; H, Hind III; and S, Sal I. (**B**) Expanded view of the region surrounding the *p35* gene. The site of the *lacZ* insertion (hatched box) is indicated, as is the extent of the deletion in vAcAnh (line beneath the genome). (A) and (B) are drawn to scale, except for the *lacZ* insert, which is 4.2 kb in length. (**C**) Nucleotide sequence and predicted amino acid sequence of the region immediately surrounding the vAcAnh deletion. The arrow indicates the junction created between position +502 of *p35* (*14*) and position −296 of *p26* (*25*) (from the initiation codons). The asterisk indicates a stop codon.

C

```
AAC CAA GTG CTA TAT GAC TCA TTT GTT TTT CAA AAC CGA ACT TGA
Asn Gln Val Leu Tyr Asp Ser Phe Val Phe Gln Asn Arg Thr  *
```

R. J. Clem, Department of Genetics, University of Georgia, Athens, GA 30602.
M. Fechheimer, Department of Zoology, University of Georgia, Athens, GA 30602.
L. K. Miller, Departments of Genetics and Entomology, University of Georgia, Athens, GA 30602.

*To whom correspondence should be addressed.

cells were undergoing an apoptosis-like response, we examined the chromatin DNA of wild-type and *p35* mutant–infected cells by agarose gel electrophoresis. A characteristic biochemical feature of apoptosis is the endonucleolytic cleavage of the cellular DNA into a chromatin ladder consisting of discrete fragments of oligonucleosomal lengths (*17*). The DNA of SF-21 cells infected with either of the two *p35* mutants, vAcAnh or vP35Z, was digested into fragments characteristic of a chromatin ladder (Fig. 3). This degradation began between 6 and 12 hours after infection and increased with time. As expected (*18*), the DNA of wild-type–infected SF-21 cells remained in a high molecular weight form over the course of the infection (Fig. 3), as did the DNA of TN-368 cells infected with the wild-type or either of the two mutants (*15*). The DNA of cells killed by freeze-thawing also remained in a high molecular weight form (Fig. 3), further indicating that *p35* mutant–induced DNA fragmentation was not simply due to rapid necrosis. In addition, cell viability, as determined by trypan blue exclusion, correlated with DNA fragmentation (legend to Fig. 3). The chromatin degradation and microscopy data (Fig. 2) indicate that premature death in *p35* mutant–infected SF-21 cells occurs by the process of apoptosis.

Thus, p35 blocks the apoptotic response that SF-21 cells mount in response to AcMNPV infection. Preliminary data indicate that p35 affects the rate at which host protein synthesis is curtailed and late viral gene expression is initiated (*15*). The transition from the early to the late phase of viral replication occurs approximately 6 hours after infection, the time at which apoptosis is initiated. Because RNA and protein synthesis are required for apoptosis to occur (*3, 4*), p35 may directly or indirectly interfere with the synthesis of cellular proteins that induce apoptosis. Transcription of *p35* occurs almost immediately on viral entry and continues throughout the course of the infection (*14, 19*). Thus, p35 is present by 6 hours after infection and may be required to maintain the block throughout the remainder of the infection process.

As determined by computer-assisted sequence analysis, the predicted p35 gene product (*14*) shares no discernible sequence relationship to any proteins in current gene databases, including the three other gene products that have been found to regulate apoptosis. Two of the genes known to regulate apoptosis, the proto-oncogene *bcl-2* and the Epstein-Barr virus latent gene *LMP 1*, block the apoptotic response of B lymphocytes by an unknown but apparently common mechanism (*20, 21*). The third gene, the tumor-suppressor gene encoding p53, induces apoptosis in a myeloid leukemic cell line, again by an unknown mechanism (*22*). All three of these genes regulate apoptosis in cells of the mammalian immune system. The *p35* gene, however, regulates apoptosis outside the immune system. Because the regulation of apoptosis is expected to be a critical factor in cell proliferation, and therefore in tumorigenesis, it will be important to identify the mechanism by which this protein controls cell death.

For the host organism, a cellular apoptotic response during viral infection probably has significant effects on viral pathogenesis. Apoptosis may have evolved as a primitive viral defense response in animals lacking humoral immune systems (*5, 23*). The amount of budded and occluded virus obtained from vAcAnh-infected SF-21 cells and of occluded virus obtained from *Spodoptera frugiperda* larvae (*15*) are dramatically reduced compared to amounts of viruses obtained in the wild-type strain. Thus, the presence of *p35* is expected to significantly increase the virulence of AcMNPV in at least some hosts. Overcoming this type of host defense response could contribute to the ability of AcMNPV to infect a broader range of insect cells.

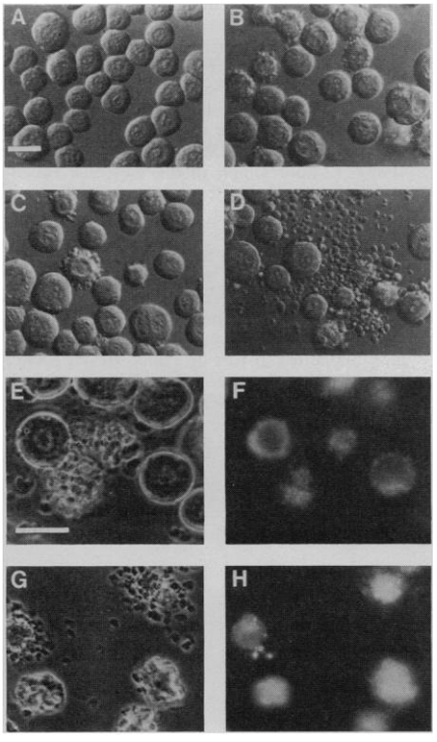

Fig. 2. Phenotype of vAcAnh at the microscopic level. (**A** to **D**) SF-21 cells were either mock-infected (A), wild-type AcMNPV-infected (B), or vAcAnh-infected (C and D) and observed at 12 hours after infection with differential interference contrast optics (*26*). Cells in early (C) and later (D) stages of blebbing are shown. Because the apoptotic response is not perfectly synchronous, some cells do not appear to be blebbing, even though <20% and <5% of the cells remain viable by 24 and 36 hours after infection, respectively (legend to Fig. 3). (**E** and **F**) Blebbing cells contain intact mitochondria, as judged by their ability to be stained with rhodamine 123. SF-21 cells infected with vAcAnh (12 hours after infection) were stained with rhodamine 123 and examined by phase-contrast (E) and flourescence (F) microscopy (*26*). The stain was confirmed to be specific for intact mitochondria by treating stained cells with the proton ionophore 2,4-dinitrophenol, which resulted in rapid destaining (*15*). (**G** and **H**) Nuclear fragmentation in blebbing cells. vAcAnh-infected SF-21 cells (12 hours after infection) were fixed, stained with the nuclear stain Hoechst G33342, and examined by phase-contrast (G) and fluorescence (H) microscopy (*26*). Bars, 20 μm.

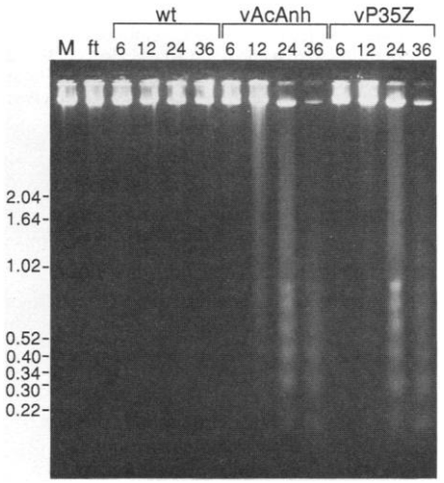

Fig. 3. Agarose gel showing DNA fragmentation in SF-21 cells infected with *p35* mutant viruses. Total DNA from mock-infected (M), freeze-thawed (ft), wild-type AcMNPV-infected, vAcAnh-infected, or vP35Z-infected cells was isolated at various times after infection, subjected to agarose gel electrophoresis, and visualized by ethidium bromide staining (*27*). Size markers are indicated to the left (in kilobases). Numbers at the top indicate hours after infection. The percentage of viable cells in each sample and the percentage of total DNA in fragments (in parentheses) was as follows (*27*): mock, 98.3% (0.0%); freeze-thawed, 1.5% (9.7%); wild type at 6 hours, 99.0% (0.0%); wild type at 12 hours, 99.2% (5.1%); wild type at 24 hours, 98.8% (7.1%); wild type at 36 hours, 97.5% (7.0%); vAcAnh at 6 hours, 98.8% (0.0%); vAcAnh at 12 hours, 62.5% (28.1%); vAcAnh at 24 hours, 17.2% (63.7%); vAcAnh at 36 hours, 4.7% (67.9%); vP35Z at 6 hours, 99.3% (0.0%); vP35Z at 12 hours, 67.6% (−7.0%); vP35Z at 24 hours, 20.2% (53.9%); and vP35Z at 36 hours, 6.5% (62.1%).

REFERENCES AND NOTES

1. J. F. R. Kerr, A. H. Wyllie, A. R. Currie, *Br. J. Cancer* **26**, 239 (1972).
2. A. H. Wyllie, J. F. R. Kerr, A. R. Carrie, *Int. Rev. Cytol.* **68**, 251 (1986).
3. N. I. Walker, B. V. Harmon, G. C. Gobé, J. F. R. Kerr, *Meth. Achiev. Exp. Pathol.* **13**, 18 (1988).
4. J. F. R. Kerr, J. Searle, B. V. Harmon, C. J. Bishop, in *Perspectives on Mammalian Cell Death*, C. S. Potten, Ed. (Oxford Univ. Press, New York, 1987), pp. 93–128.

5. E. Martz and D. M. Howell, *Immunol. Today* **10**, 79 (1989).
6. R. A. Lockshin, in *Comprehensive Insect Physiology Biochemistry and Pharmacology*, G. A. Kerkut and L. I. Gilbert, Eds. (Pergamon, Elmsford, NY, 1985), vol. 2, pp. 301–317.
7. W. A. Smith and H. F. Nijhout, *Tissue Cell* **14**, 243 (1982).
8. N. Pipan and V. Rakovec, *Zoomorphologie* **94**, 217 (1980).
9. F. Giorgi and P. Deri, *J. Embryol. Exp. Morphol.* **35**, 521 (1976).
10. L. K. Miller, *Annu. Rev. Microbiol.* **42**, 177 (1988).
11. J. L. Vaughn, R. H. Goodwin, G. J. Tompkins, P. McCawley, *In Vitro* **13**, 213 (1977).
12. L. E. Volkman and P. A. Goldsmith, *Appl. Environ. Microbiol.* **44**, 227 (1982).
13. W. F. Hink, *Nature* **226**, 466 (1970).
14. P. D. Friesen and L. K. Miller, *J. Virol.* **61**, 2264 (1987).
15. R. J. Clem and L. K. Miller, unpublished results
16. L. B. Chen, *Methods Cell Biol.* **29**, 103 (1989).
17. A. H. Wyllie, *Nature* **284**, 555 (1980).
18. M. E. Wilson and L. K. Miller, *Virology* **151**, 315 (1986).
19. M. S. Nissen and P. D. Friesen, *J. Virol.* **63**, 493 (1989); J. A. Dickson and P. D. Friesen, *ibid.* **65**, 4006 (1991).
20. D. Hockenberry, G. Nunez, C. Milliman, R. D. Schreiber, S. J. Korsmeyer, *Nature* **348**, 334 (1990).
21. S. Henderson *et al.*, *Cell* **65**, 1107 (1991).
22. E. Yonish-Rouach *et al.*, *Nature* **352**, 345 (1991).
23. W. M. Clouston and J. F. R. Kerr, *Med. Hypotheses* **18**, 399 (1985).
24. The vAcAnh mutation was mapped to the Eco RI-S fragment (86.7 to 87.9 map units) by cotransfection of SF-21 cells with vAcAnh DNA and a series of recombinant λ DNAs containing the entire wild-type (L-1 strain) [H. H. Lee and L. K. Miller, *J. Virol.* **27**, 754 (1978)] AcMNPV genome in overlapping segments. The vAcAnh Eco RI-S fragment was cloned into pBluescript (Stratagene, La Jolla, CA) and sequenced by the dideoxy chain termination method with Sequenase (U.S. Biochemical Corp., Cleveland, OH). vP35Z was constructed by replacing the Bcl I–Sal I fragment of *p35* with a Bam HI–Sal I fragment from plasmid pMC874 [M. J. Casadaban, J. Chou, S. N. Cohen, *J. Bacteriol.* **143**, 971 (1980)], which contained the *lacZ* gene. The resulting recombinant plasmid, which had *lacZ* fused in-frame to the NH_2-terminus of *p35*, was used to construct the recombinant virus vP35Z by cotransfection of TN-368 cells with wild-type DNA. vP35Z was identified as a blue plaque in the presence of 5-bromo-4-chloro-3-indolyl β-D-galactopyranoside (X-gal) and its DNA was characterized by restriction endonuclease analysis and Southern (DNA) blotting.
25. M. A. Cochran and P. Faulkner, *J. Virol.* **45**, 961 (1983); L. A. Guarino and M. D. Summers, *ibid.* **60**, 215 (1986); A. Liu, J. Qin, C. Rankin, S. E. Hardin, R. F. Weaver, *J. Gen. Virol.* **67**, 2565 (1986).
26. SF-21 cells were grown on cover slips in microscope chambers and infected [D. R. O'Reilly and L. K. Miller, *J. Virol.* **62**, 3109 (1988)] at a multiplicity of infection of 20 plaque-forming units per cell on the basis of titers obtained in TN-368 cells. All images were obtained with a Zeiss IM 35 fluorescence microscope and Kodak Tri-X film. Differential interference contrast images were recorded with a ×63 [numerical aperture (NA) 1.4] planapo objective. Phase contrast and fluorescence images were recorded with a ×100 (NA 1.4; PH3) neofluar objective. Cells were stained with rhodamine 123 (Molecular Probes, Eugene, OR) (*16*) and observed with the fluorescein (#487710) filter set. For nuclear staining, cells were grown on coverslips and fixed with 3.7% formaldehyde in phosphate-buffered saline (PBS), pH 7.5, for 15 min at room temperature, then incubated in cold (−20°C) acetone 3 min, air-dried, and stored at −20°C until stained. Fixed cover slips were stained with 10 μM Hoechst 33342 (Molecular Probes) in PBS (pH 7.5) overnight at room temperature in the dark and were observed with the ultraviolet (#487702) filter set.
27. SF-21 cells were infected as above (*26*) but with 60-mm tissue culture plates. After the indicated number of hours, the cells (4×10^6 per sample) were lysed in 0.4 M tris (pH 7.5), 0.5 M EDTA, 0.1% SDS, and 200 μg ml^{-1} proteinase K for 6 hours at room temperature. The lysates were phenol extracted and ethanol precipitated. Half of each sample was loaded on a 1.2% agarose gel and separated by electrophoresis overnight at 50 volts in buffer containing ethidium bromide. The gel was then treated for 4 hours with 20 μg ml^{-1} ribonuclease A in running buffer with ethidium bromide at room temperature. Freeze-thawed cells were subjected to three 5-min cycles in liquid nitrogen and a 37°C water bath before DNA isolation. To determine cell viability, we stained cells with 0.04% trypan blue in culture medium. Intact cells that excluded the dye were counted as viable, and the percentage of viable cells that remained was determined based on the original number of cells (approximately 1000) per unit volume. To determine the percentage of DNA in fragments, we scanned a Polaroid negative of the gel with Molecular Dynamics Computing Densitometer Model 300A and ImageQuant version 3.0. The lane containing the freeze-thawed cells was normalized to the mock lane, and lanes containing virus-infected cells were normalized to the 6-hour lane. The amount of DNA fragmentation in the vP35Z 12-hour sample in this particular experiment was atypical, as it was normally similar to vAcAnh at 12 hours.
28. We thank R. Russnak for the gift and the naming of the annihilator mutant, B. G. Ooi for preliminary characterization of the mutant, S. Maeda and T. Morris for the BmN-4 cell line, D. O'Reilly for many insightful comments and suggestions, and S. Hilliard and J. Todd for excellent technical assistance. Supported in part by Public Health Service Grant AI23719 from the National Institute of Allergy and Infectious Diseases to L.K.M.

7 June 1991; accepted 13 September 1991